



Review

Standardless quantification methods in electron probe microanalysis

Jorge Trincavelli ^{a,b,*}, Silvina Limandri ^{a,b}, Rita Bonetto ^c^a Facultad de Matemática, Astronomía y Física, Universidad Nacional de Córdoba, Ciudad Universitaria, 5000 Córdoba, Argentina^b Instituto de Física Enrique Gaviola, Consejo Nacional de Investigaciones Científicas y Técnicas de la República Argentina, Medina Allende s/n, Ciudad Universitaria, 5000 Córdoba, Argentina^c Centro de Investigación y Desarrollo en Ciencias Aplicadas Dr. Jorge Ronco, Consejo Nacional de Investigaciones Científicas y Técnicas de la República Argentina, Facultad de Ciencias Exactas, de la Universidad Nacional de La Plata, Calle 47 N° 257, 1900 La Plata, Argentina

ARTICLE INFO

Article history:

Received 24 April 2014

Accepted 26 July 2014

Available online 2 August 2014

Keywords:

Standardless analysis

Electron probe microanalysis

Quantification methods

Estimation of uncertainties

ABSTRACT

The elemental composition of a solid sample can be determined by electron probe microanalysis with or without the use of standards. The standardless algorithms are quite faster than the methods that require standards; they are useful when a suitable set of standards is not available or for rough samples, and also they help to solve the problem of current variation, for example, in equipments with cold field emission gun. Due to significant advances in the accuracy achieved during the last years, product of the successive efforts made to improve the description of generation, absorption and detection of X-rays, the standardless methods have increasingly become an interesting option for the user. Nevertheless, up to now, algorithms that use standards are still more precise than standardless methods. It is important to remark, that care must be taken with results provided by standardless methods that normalize the calculated concentration values to 100%, unless an estimate of the errors is reported. In this work, a comprehensive discussion of the key features of the main standardless quantification methods, as well as the level of accuracy achieved by them is presented.

© 2014 Elsevier B.V. All rights reserved.

Contents

1.	Introduction	77
2.	Advances in the description of generation, attenuation and detection of X-rays	77
2.1.	X-ray generation	77
2.1.1.	Bremsstrahlung	77
2.1.2.	Characteristic X-rays	78
2.2.	X-ray attenuation	78
2.3.	X-ray detection	78
2.3.1.	Energy dispersive spectrometers (EDS)	78
2.3.2.	Wavelength dispersive spectrometers (WDS)	78
3.	Standardless analysis	78
3.1.	Database methods	79
3.2.	P/B methods	79
3.2.1.	Lábár and Török model	79
3.2.2.	Trincavelli and Van Grieken method	79
3.2.3.	Heckel and Jugelt model	79
3.3.	MC methods	79
3.3.1.	Reverse Monte Carlo algorithm	80
3.3.2.	XRF-EPMA unified Monte Carlo approach	80
3.4.	Variable take-off method	80
3.5.	Fundamental methods	80
3.5.1.	Wernisch model	80
3.5.2.	DTSA package	81
3.5.3.	Fournier model	81

* Corresponding author at: Facultad de Matemática, Astronomía y Física, Universidad Nacional de Córdoba, Medina Allende s/n, 5000 Córdoba, Argentina. Tel.: +54 351 4334051; fax: +54 351 4334054.

E-mail addresses: trincavelli@famaf.unc.edu.ar (J. Trincavelli), s.limandri@conicet.gov.ar (S. Limandri), bonetto@quimica.unlp.edu.ar (R. Bonetto).

3.5.4.	Horny et al. method	81
3.5.5.	Limandri et al. method	81
4.	Precision and accuracy of the different methods	82
4.1.	Individual particles	82
4.2.	Bulk samples	82
5.	Conclusion	83
	References	84

1. Introduction

The technique known in our days as electron probe microanalysis (EPMA) was developed by Raymond Castaing in the middle of the last century [1,2]. This non-destructive technique for chemical characterization is based on the analysis of the X-ray spectrum emitted when a sample is irradiated by an electron beam. In its original version, a wavelength dispersive spectrometer (WDS) was used for the detection of X-rays. An important change was introduced in 1968 with the Si(Li) X-ray detectors [3], which gave rise to the energy dispersive spectrometers (EDS). They are faster, more stable and more efficient than the crystal spectrometer, although an important loss in resolution has to be paid.

To obtain the mass concentrations C_j , conventional EPMA involves the use of standards. In this case, the intensity $P_{j,q}$ of the characteristic line q emitted by each element j of an unknown sample is compared with the corresponding intensity $P_{j,q,0}$ emitted from a standard with concentrations $C_{j,0}$.

$$\frac{C_j}{C_{j,0}} = \frac{P_{j,q}}{P_{j,q,0}} \cdot \mathbf{ZAF} \quad (1)$$

Thus, to obtain the unknown concentrations, the intensity ratios $k_j = P_{j,q}/P_{j,q,0}$ must be corrected by matrix effects, denoted as **ZAF** correction factors, i.e., effects related to all the elements present in the sample and in the standard. Thus, production (**Z**), absorption (**A**) and enhancement of the characteristic radiation (**F**) must be taken into account. Two groups of methods have been extensively used to carry out these corrections: the models based on the **ZAF** factors and the ones which use the ionization distribution function $\varphi(\rho z)$ [4,5]. According to the last formulation,

$$\mathbf{ZA} = \frac{\int_0^\infty \varphi(\rho z) e^{-\mu \text{csc}\theta/\rho z} d\rho z}{\int_0^\infty \varphi_0(\rho z) e^{-\mu_0 \text{csc}\theta/\rho z} d\rho z}$$

where μ is the mass absorption coefficient for the analyzed energy and ψ is the take-off angle formed between the direction of the X-rays in their way to the detector and the sample surface. The subindex 0 refers to the standard.

These models have been proposed for different types of samples, leading to a progressive improvement in EPMA precision. The relative uncertainties are about 5% for major and minor elements, i.e., with concentrations greater than 10% and between 1 and 10%, respectively, and somewhat greater for trace elements (concentrations lower than 1%) [6]. Mineral samples constitute a special case for which, provided the adequate standards are available, the relative errors of the elemental concentrations are lower than 2% in most of the typical situations [7].

The main inconvenience of the methods described is that they require the measurement of a proper set of standards, which must be suitable for the particular sample studied. This requirement comprises two obvious conditions: first, an adequate set of standards must be available, and second, whole spectra or at least, some values at specific energies, must be measured for each standard to determine the net characteristic peak intensities. Usually, the unknown and standards must be measured in the same conditions, which imply that all measurements

should be performed close in time. Otherwise, changes in detector efficiency and filament emission rate, among other possible parameters, could become significant sources of error. On the other hand, an important advantage related to the use of standards is that several atomic and experimental parameters cancel out in the k ratio, which reduces the uncertainty of the concentrations obtained.

According to Gauvin [8] and to our own experience, despite its good precision, quantitative X-ray microanalysis with standards is not used by most of the microscopists who acquire EDS spectra in electron microscopes. In fact, most of the samples of interest are not perfectly homogeneous and flat, as required by the current models. In addition, a proper set of standards is not always available. For these reasons, a compromise must be done between an ideal accurate quantification with standards, and a standardless method actually applicable to the particular situation. To optimize this compromise, a great effort has been done to improve [9–15] and develop [6,16–24] standardless algorithms in the last thirty years. Summarizing the advantages of standardless analysis, the main and obvious one is that they are not constrained to the samples for which a proper set of standards is available, besides, they are less time-consuming and some of the methods can be used for irregular samples.

The main disadvantage of the standardless methods of analysis in EPMA, as compared to the conventional ones, is that several fundamental and instrumental parameters must be known to obtain results with reasonable precision, particularly for the methods based on first principles (see below). Thus, the physics underlying generation, propagation and detection of X-rays must be properly known. Therefore, adequate descriptions of characteristic radiation, bremsstrahlung, and detection artifacts are required.

2. Advances in the description of generation, attenuation and detection of X-rays

The improvement of the accuracy and precision of standardless quantification methods in EPMA is related to the advances performed to improve the description of generation, propagation and detection of X-rays. In addition, the development of silicon drift X-ray detectors contributed to the quality of both conventional and standardless EPMA analysis. The main achievements in those fields are shortly described in this section.

2.1. X-ray generation

2.1.1. Bremsstrahlung

In the last two decades, several advances were produced in the description of the continuous X-ray spectrum generated by 1–40 keV electrons. Three different kinds of approaches have been faced to study the bremsstrahlung behavior as a function of the atomic number and the incident energy: theoretical calculations, Monte Carlo simulations and empirical fitting. Theoretical models are based in the assessment of a numerical integration involving the bremsstrahlung differential cross section [25,26] as a function of the photon energy. In this sense, Ambrose et al. [27] developed a model for the thick target bremsstrahlung that was later applied by Semaan and Quarles [28] to describe the continuum spectrum obtained with a scanning electron microscope. On the other

hand, bremsstrahlung spectra induced by keV electron impact have also been obtained from Monte Carlo simulations [29,30]. Finally, a number of empirical expressions, mainly for normal incidence, have been suggested to give an analytical description of the bremsstrahlung spectrum in EPMA [31–33]. A more detailed description of this subject is given elsewhere [34].

2.1.2. Characteristic X-rays

The generation of X-ray characteristic peaks involves different ionization and relaxation processes which have been extensively investigated. Particularly, magnitudes like ionization cross sections, fluorescence yields, relative transition probabilities, as well as the description of satellite lines are continuously studied.

In the case of K shell ionization cross section by electron impact, a number of recent results are available. Particularly, several theoretical approaches were developed; some of them are based on the binary-encounter Bethe (BEB) model [35], other ones, on the partial wave first Born approximation (PWBA) [36–39], and other ones, on the distorted wave first Born approximation (DWBA) [38,40,41]. In addition, semi-empirical expressions [42–44] and experimental data [45–49] were obtained during the last years.

L shell ionization cross sections are more difficult to obtain, particularly experimental data, because fluorescence yields and Coster–Kronig transition rates are poorly known; nevertheless, some analytical expressions [12,38] and theoretical approaches [40,50–52] were recently developed; in addition, a number of experimental determinations of X-ray production and ionization cross sections [53–59] were carried out, as reviewed by Llovet et al. [60].

Regarding M lines, few experimental data are available for ionization cross sections [61–64]. On the other hand, some of the theoretical formalisms developed for K and L shells are also valid for M shells [38,50,51].

Relative transition probabilities are also required to perform standardless quantification, especially when L and M lines are involved. For L decay rates of elements with $30 \leq Z \leq 92$, Puri [65] computed X-ray line intensities relative to the most intense line in each subshell from published X-ray emission rates based on the Dirac–Fock model. On the other hand, several experimental determinations were carried out, although for certain specific elements or transitions [66–72].

Regarding M shell relative transition probabilities, theoretical calculations were performed by Chen and Crasemann for elements in the range $48 \leq Z \leq 92$ [73] and by Puri for elements with $65 \leq Z \leq 92$ [65]. Experimental determinations are very scarce [74] and cannot be used to construct a database for standardless quantification.

Fluorescence yield coefficients ω and Coster–Kronig transition probabilities f_{ij} are parameters particularly important for standardless methods when L or M lines are used for quantification. In fact, they impose a severe restriction to the reliability of quantitative results, because large errors are associated with these magnitudes. Uncertainties up to 35% can be expected for ω_{L1} [75] and 5% for ω_{L2} and ω_{L3} [76], while errors are around 20% for f_{13} and from 20% to 100% for f_{12} , depending on the atomic number [75]. For f_{23} the errors can reach 25% [76]. Even more critical are M shell parameters, for which no reliable error estimation can be performed until experimental data is available [77].

2.2. X-ray attenuation

The X-ray attenuation within the unknown sample (self-absorption) is mainly ruled by the photoelectric cross sections in the energy range usual for EPMA. In this sense, the level of accuracy of mass absorption coefficients (MACs) is important for standardless methods, although these coefficients are not as critical as ionization cross sections, relative transition probabilities, fluorescence yields and Coster–Kronig transition rates (in the case of L and M lines). Particularly, peak-to-background based standardless algorithms have a lower dependence (if any) on MACs. A comprehensive database of mass absorption coefficients was

semiempirically determined and tabulated by Henke et al. [78] and also by Chantler from a theoretical approach [79].

2.3. X-ray detection

The efficiency curve of the spectrometer used is required to perform standardless quantification, except for peak-to-background ratio based standardless algorithms.

2.3.1. Energy dispersive spectrometers (EDS)

The response of these spectrometers is, in principle, easy to predict in terms of the detector window, the contact layer and the dead layer mass thicknesses; nevertheless these thicknesses are not always well known, particularly regarding the dead layer. In addition, for detectors with ultrathin windows, a supporting grid acts partially shadowing the X-rays; thus, both the efficiency for photons passing through the grid material, and the energy independent efficiency for photons passing through the grid holes must be properly taken into account [14]. Finally, an ice or contamination layer can also be present, and its evolution with time should be periodically monitored.

2.3.2. Wavelength dispersive spectrometers (WDS)

The efficiency curve of a WDS is more difficult to predict, because it depends on the quantum efficiency of the proportional counter, on geometrical factors and on the reflectivity of the analyzing crystal. Different methods were developed to determine the efficiency of a WDS: one of them involves the measurement of characteristic line intensities of pure elements [18], other methods are based on the comparison of an experimental spectrum measured in a region free of characteristic lines and the analytical prediction [80] or the Monte Carlo simulation [81] of the corresponding bremsstrahlung. A different approach consists in the comparison of spectra measured from the same sample, one of them with the WDS whose efficiency curve is searched and the other one with an EDS of known efficiency [14].

3. Standardless analysis

The magnitudes mentioned in the previous section influence the precision of standardless quantification procedures. Realistic models for the description of ionization cross section, for instance, those based on DWBA, present uncertainties around 5% for K lines [24], and greater for L and M lines. On the other hand, the spectrometer efficiency, not required for analysis involving standards, becomes an important factor in some standardless algorithms. For example, the uncertainties in the efficiency of a particular silicon drift detector have been estimated to be around 10% in the energy range between C-K and O-K lines, around 1% at the Al-K α characteristic energy and 0.2% at Ti-K α [49].

In the case of standardless procedures based on first principles, the main sources of error are related to the uncertainties associated with the measured intensities, especially for trace elements, the knowledge of atomic parameters and the description of the detection efficiency in the low energy region. Finally, it must be stated that some of the standardless methods normalize the concentrations to 100%, masking possible errors.

Summarizing, as stated by Newbury et al., it is potentially dangerous to report the concentration values obtained by a standardless method without the corresponding uncertainties. Particularly, these uncertainties should take into account not only the statistics associated with the experimental data, but also the errors involved in the different parameters and functions present in the method used; otherwise, “any numerical value reported will be assumed to be absolutely true by subsequent users of the result” [6]. Nevertheless, the precision of standardless methods have improved noticeably during the last years [82], as will be discussed in Section 4.

The standardless methods can be classified into five different groups: methods involving databases or stored standards (they will be

referred to as database methods), algorithms based on peak-to-background ratios (P/B), methods developed on the basis of Monte Carlo simulations (MC), microanalysis with variable take-off angle (variable take-off), and procedures mainly consisting on the application of fundamental equations of microanalysis (fundamental methods). The following section will deal with these five types of standardless algorithms of EPMA quantification, for which some examples available in the literature will be discussed.

3.1. Database methods

In these methods, typically used by commercial packages, a database of characteristic intensities is created from a set of experimental spectra, usually mono-elemental standards measured under different excitation conditions [6,24]. To complete the database, those intensities are mathematically interpolated for elements or conditions not measured. The complete set of stored standards (experimental and interpolated) is used to determine the k ratios. The reliability of this kind of methods lies on the completeness of the database and leads to inaccurate results when the interpolation is not adequate. In addition, these methods usually normalize the concentration values to 100%.

3.2. P/B methods

Algorithms based on peak-to-background calculations rely on the assumptions that both characteristic and bremsstrahlung photons are originated in a similar region of the sample and that bremsstrahlung is emitted almost isotropically [19]. With these assumptions, the absorption corrections for characteristic radiation and bremsstrahlung can be considered the same and they cancel out. These methods are inspired on the ideas originally (and independently) suggested by Small et al. [83] and by Statham and Pawley [84]. Nevertheless, the original versions of the P/B methods require the use of standards.

One important advantage of P/B methods is that they do not depend on the detector efficiency, because it is exactly the same for the characteristic X-rays and the bremsstrahlung photons of the same energy. In addition, in principle, there is no need for a normalization step, as mentioned by Lábár and Török [17]. Thus, the sum of the calculated concentrations can be used as a quality criterion for the analysis or to obtain a non-detectable element, like hydrogen. Nevertheless, the results presented by these authors are normalized to 100%, as in the case of Trincavelli and Van Grieken algorithm [19], while Heckel and Jugelt [16] method does not require normalization.

3.2.1. Lábár and Török model

Lábár and Török [17] developed a method based on the use of K ratios, being $K = (P/B)_{\text{unk}}/(P/B)_{\text{std}}$ the quotient between the peak-to-background ratios for the unknown and a pure standard, for each particular characteristic line. The mass concentrations can be calculated as

$$C_j = K_{j,q} \cdot Z_c A_c F_c R_c$$

The subindexes j and q have the same meaning as in Eq. (1); Z_c , A_c , F_c , and R_c are corrections to account for the differences in the generation, absorption, secondary fluorescence and backscattering losses of characteristic and bremsstrahlung radiation, although backscattering and absorption effects are treated as second order corrections and fluorescence effects are disregarded.

In this formalism, $(P/B)_{\text{std}}$ can be calculated using some of the models available for the prediction of characteristic peaks and bremsstrahlung; particularly, the authors recommend Pouchou and Pichoir's equations [85] for the former along with the model proposed by Small et al. [86] for the latter.

3.2.2. Trincavelli and Van Grieken method

The model proposed by Trincavelli and Van Grieken [19] does not involve the calculation of peak-to-background ratios in hypothetical standards, but a direct computation of the mass concentrations based on the measurement of the $P_{j,q}$'s:

$$P_{j,q} = C_j (ZAF)_j \omega_j p_{j,q} \varepsilon_{j,q} I t \frac{\Delta\Omega}{4\pi} \quad (2)$$

and the bremsstrahlung $B_{j,q}$ in the corresponding energy windows:

$$B_{j,q} = f(\bar{Z}, E_{j,q}, E_0) A \varepsilon_{j,q} I t \frac{\Delta\Omega}{4\pi} \quad (3)$$

where ω is the fluorescence yield and p is relative transition probability; Z , A , and F account for the atomic number, absorption and secondary fluorescence matrix corrections related to the production of characteristic X-rays; f describes the generation of bremsstrahlung, being a function of the mean atomic number \bar{Z} of the sample, characteristic energy E and the incidence energy E_0 ; ε is the spectrometer intrinsic efficiency, I is the beam current, t is the acquisition time, and $\Delta\Omega$ is the solid angle subtended by the detector. It must be noted that these ZAF factors are not related to similar corrections in adequate standards, as the conventional ZAF corrections. From Eqs. (2) and (3), the mass concentrations can be easily derived:

$$C_j = \frac{P_{j,q}}{B_{j,q}} \frac{f(\bar{Z}, E_{j,q}, E_0)}{(ZF\omega p)_{j,q}} \quad (4)$$

The factor A does not appear in Eq. (4) because the X-ray absorption is supposed to be similar for both characteristic and bremsstrahlung photons of the same energy, as mentioned before.

Both standardless P/B methods discussed up to here were designed to characterize small particles and rough samples, although they are also appropriate for polished bulk samples.

3.2.3. Heckel and Jugelt model

Heckel and Jugelt [16] developed a standardless method for the quantitative analysis of bulk samples. According to this formalism, the mass concentrations can be obtained iteratively from the following relation:

$$\frac{P_{j,q}}{B_{j,q}} = C_j \omega_j p_{j,q} V_S V_R V_f F_{j,q} \quad (5)$$

where V_S is the ratio between a generation factor for characteristic radiation and bremsstrahlung (mainly depending on the stopping power and the corresponding cross section), and V_R and V_f are similar ratios for backscattering losses and self-absorption correction factors, respectively.

Both V_R and V_f depend on the mass concentrations, and were studied by means of Monte Carlo simulations, leading to the conclusion that these factors are different from 1. Particularly, V_f is expressed in terms of the factor L , i. e., the path length of the photons within the sample traveling to the detector, relative to their generation depth. By variation of L , consistency between calculated and measured background is achieved.

This model was the basis of a further development for spectra simulation [87], that is to say, the reverse way from a known sample composition to the X-ray emission spectrum.

3.3. MC methods

There is certain arbitrariness in the classification of these methods, because several algorithms use expressions based on Monte Carlo simulations at a different extent. For instance, according to Newbury et al.

[6], in the standardless program Desktop Spectrum Analyzer (DTSA) [88], energy losses due to backscattered electrons were accounted for using an expression derived from Myklebust and Newbury [89], which is based on the Monte Carlo formalism. Simulations were also used by Horny et al. [23] to compute the net X-ray intensity of a characteristic line of the interest element emitted from a thick specimen. Heckel and Jugelt [16] use Monte Carlo to assess the ratio of backscatter correction factors and the ratio of absorption correction factors, related to characteristic and continuous radiation. Nevertheless, the standardless algorithms referred to in the present review as MC methods are the ones completely based on Monte Carlo simulations.

3.3.1. Reverse Monte Carlo algorithm

The approach developed by Ro et al. [21] performs a reverse Monte Carlo simulation schedule in which successive iterations are carried out to quantify individual particles by an energy dispersive spectrometer in EPMA. In each iteration step, simulated characteristic X-ray intensities are compared with those measured, generating a new set of approximate concentration values for the chemical elements in the particle. When the simulated X-ray intensities converge to the experimental ones, the input values of elemental concentrations used for this last simulation, normalized to 100%, determine the chemical composition of the sample. In their method, the authors carried out a modification of the CASINO software package for Monte Carlo simulation of electron trajectories in solids [90] for the application to spherical, hemispherical and hexahedral particles on a flat surface.

The reverse Monte Carlo approximation is used to find the solution of the following set of nonlinear equations:

$$P_{j,q,meas} = p_{ms} P_{j,q,sim} (C_{1,q}, C_{2,q}, \dots, C_{n,q}, d, \rho) \quad j = 1, \dots, n$$

$$\text{and} \quad \sum_{j=1}^n C_j = 1$$

where n is the number of chemical elements in the sample, and the sub-indexes *meas* and *sim* refer to the measured and simulated intensities, respectively. The factor p_{ms} includes instrumental parameters, ρ and d represent the mass density and any characteristic dimension of the particle.

In this algorithm it is assumed that: (i) the particle material is homogeneous; (ii) all of the elements in the sample are detected except H, Li, Be, and B; (iii) the particle is placed on a flat surface of known composition; and (iv) the shape of the analyzed particle is spherical, hemispherical, or hexahedral.

3.3.2. XRF–EPMA unified Monte Carlo approach

In this approach both X-ray fluorescence and electron probe analysis are performed in the scanning electron microscope. The XRF analysis is achieved by using a special sample holder with a thin removable molybdenum target placed on top of the sample. The electron beam enters into the holder through an aperture and impinges onto the target foil which acts as an anode. A filter is used to eliminate the electrons transmitted through the Mo foil and the X-rays generated in the foil are used to excite the sample. To acquire electron excited spectra, the foil is removed [22].

A probabilistic Monte Carlo model based on first principles is implemented, which involves X-ray and electron single scattering and subsequent processes occurring with sample atoms. Particularly, the inner shell ionization cross sections are taken from Gryzinski [91], while Kramers cross sections are used to predict the generation of continuous X-rays.

By convolution with the detector response function (assumed to be Gaussian), the generated X-rays are converted into a simulated spectrum which is subsequently scaled to experimental data. The best fit between experimental and simulated spectra in multielement samples is achieved by iteratively adjusting the composition.

Detection limits are improved by the use of both electron and X-ray excited spectra. X-ray fluorescence analysis in the scanning electron microscope greatly improves the signal to background ratios of medium and high atomic number elements whereas electron probe microanalysis is more sensitive towards light elements.

3.4. Variable take-off method

The method called TWIX, developed by Völkerer et al. [92,93] is based on a correction model for oblique angle of incidence. The X-ray path lengths in samples at different take-off angles are used to find the sample composition. To this end, two spectra are measured with the sample tilted in a suitable angle for two different azimuth angles: one of them obtained by a horizontal rotation of 180° with respect to the other one. The calculated ratio of X-ray intensities k_{theo} , corresponding to the two mentioned configurations can be written for each characteristic peak as

$$k_{theo} = \frac{\int_0^{\infty} \varphi(\rho z) e^{-\mu \csc(\psi+\gamma)\rho z} d\rho z}{\int_0^{\infty} \varphi(\rho z) e^{-\mu \csc(\psi-\gamma)\rho z} d\rho z} \quad (6)$$

where ψ refers to the take-off angle with respect to the non tilted (horizontal) sample holder plane and γ is the tilt angle.

The mass concentrations implicitly present in Eq. (6) through the ionization distribution function and the mass absorption coefficient of the sample are iteratively obtained by minimizing the difference between k_{theo} and the experimental ratio k_{exp} . The novelty of this method is that performing the ratio k_{theo} , the evaluation of a number of atomic and instrumental parameters not well known is avoided. This method is also used for thickness determination of thin films.

3.5. Fundamental methods

Different approaches have been implemented to face the problem of standardless quantification in the frame of first principles. Some of these methods determine the sample composition using the characteristic intensities calculated from fundamental equations [6,18]. Another method uses a similar approach although also involves the use of data previously stored [20]. In addition, a method involving the ratio of the characteristic intensities of two elements present in the sample was developed to solve the problem of current fluctuations in a cold field emission gun scanning electron microscope (FEG-SEM) [23]. Finally, a different approach uses the whole spectrum to obtain the elemental concentrations in a formalism of parameter optimization [24]. Although not intrinsically necessary for this kind of methods, all the models described in the following subsections normalize the concentration values to 100%.

3.5.1. Wernisch model

As Wernisch pointed out, quantitative analysis based on a comparison with standards of known composition is not always possible [18]. This author gave three common problems in performing such a comparison: first, the composition of the standards at the microscopic scale is not necessarily identical with the bulk nominal composition; second, the wide range of standards required to cover all the possible applications is not always available; third, certain standards tend to evaporate or oxidize very rapidly. Even when the standard manufacturer may assure their homogeneity at microscopic scale, and avoiding unstable materials, the second issue cannot be overcome by conventional quantification routines.

In the Wernisch model, the concentrations can be obtained iteratively from the equation

$$C_j = \frac{P_{j,q}}{\varepsilon_{j,q} G_{j,q}(\bar{C})} \quad (7)$$

where $\varepsilon_{j,q}$ is the spectrometer efficiency for the characteristic energy $E_{j,q}$, and the function $G_{j,q}$ depends on the whole set of concentrations \bar{C} through the sample stopping power, and through factors due to absorption and characteristic fluorescence enhancement. The backscatter losses were omitted from the evaluation of Eq. (7). This equation can be solved iteratively starting from initial values calculated as normalized net intensities and with the condition that all the concentrations add to one. The stopping power used is based on the model given by Love et al. [94] and the absorption factor is taken from ref. [95].

3.5.2. DTSA package

The Desktop Spectrum Analyzer (DTSA) package developed by C. Fiori et al. at the National Institute of Standards and Technology and the National Institute of Health in the '80s and early '90s was developed on the same bases as the Wernisch method, although both use different models for the parameters and expressions involved, and in DTSA the backscatter losses were properly taken into account. This approach uses the stopping power proposed by Pouchou and Pichoir [96], the absorption factor developed by Heinrich and Yakowitz [97] and backscatter losses taken from the work of Myklebust and Newbury [89]. In addition, the program allows the user to choose the ionization cross section separately for the K-, L, and M-shells from a wide variety of published cross sections [6].

DTSA calculates the intensity emitted from a pure element hypothetical sample by means of the following equation

$$P_{j,q,pure} = \frac{\omega_j N_0 \rho_j R}{A_j} \int_{E_0}^{E_c} \frac{Q_j}{(-dE/ds)} dE \quad (8)$$

where N_0 is Avogadro's number, R is the backscatter loss factor, A_j is the atomic weight of element j , E_c is the critical ionization energy for the shell of interest, Q_j is the ionization cross section of element j , and dE/ds is the rate of energy loss due to inelastic scattering.

A k-ratio is calculated for each constituent by dividing its experimental intensity in the unknown by the corresponding theoretical standard intensity given by Eq. (8). After k-values for all the elements are calculated, the ZAF matrix correction procedure is performed as usual. This software package was extensively described and assessed by Newbury et al. [6].

3.5.3. Fournier model

Even when the model proposed by Fournier et al. [20] cannot be strictly classified as a fundamental method, it is considered in this section because it computes intensities corresponding to standards from calculations based on the description of radiation-matter interaction processes, when reference peaks have not been previously acquired; otherwise, reference values are extracted from a base of measured data. For the calculations, the $\varphi(\rho z)$ model proposed by Merlet [98] is used, along with Bethe ionization cross section [99]:

$$P_{j,q} = C_j I t \frac{\Delta\Omega}{4\pi} \varepsilon p_{j,q} (1 + g_{ck}) F \frac{N_0}{A_j} Q_j(E_0) \int_0^\infty \varphi(\rho z) e^{-\mu \text{csc}(\psi) \rho z} d\rho z$$

The factor $(1 + g_{ck})$ accounts for all the relevant Coster–Kronig contributions. The fluorescence yields given by Bambynek [100] for the K-shell and by Hubbell et al. [101] for L- and M-shells were used. In addition, the authors suggest two different methods to determine the WDS efficiency curve. Unfortunately, this standardless method was tested only in two samples: andradite [20] and $\text{UO}_2\text{-ZrO}_2$ [102].

3.5.4. Horny et al. method

The use of standards in EPMA quantification procedures requires that all the experimental conditions remain the same during the measurements of the sample and standards; nevertheless, this condition is not fulfilled for cold FEG-SEMs, for which beam current can fluctuate around 5% in its stable regime. This problem encouraged Horny et al. [23] to carry out an alternative to standardless quantitative X-ray microanalysis. This method is based on the Cliff–Lorimer [103] procedure originally proposed for the analytical transmission electron microscope.

The problem of current fluctuation and the corrections for X-rays generated from thick specimens are faced using the ratio of the characteristic intensities of two elements in the sample. Effects not properly taken into account in the generation, absorption and detection of X-rays are accounted for a calibration factor that must be calculated from characteristic intensities previously measured from a standard. Nevertheless, the calculation of the emitted X-ray characteristic intensity of the interest elements cannot be avoided and was performed by Monte Carlo simulations. For this purpose, the authors developed a program using the single scattering approach of Gauvin et al. [104]. This method was presented by the authors as a sketch of the required steps to perform reliable standardless X-ray microanalysis.

3.5.5. Limandri et al. method

A different approach was faced recently [24], based on the ideas developed originally by Rietveld for X-ray diffraction [105–107] and adapted for EPMA by Bonetto et al. [108]. The method consists in minimizing the χ^2 parameter, which represents the quadratic differences between an experimental spectrum and an analytical function proposed to describe it, by optimization of the parameters involved in the analytical prediction:

$$\chi^2 = \frac{1}{N_c - N_p} \sum_{i=1}^{N_c} \frac{(\tilde{I}_i - I_i)^2}{I_i}$$

where I_i and \tilde{I}_i are, respectively, the experimental and calculated intensities corresponding to the channel i , N_c is the total number of channels and N_p is the number of parameters to be refined.

This algorithm, implemented in the software POEMA (Parameter Optimization in Electron Probe Microanalysis), allows for the determination of the elemental concentrations, along with an estimation of their errors. To this end, uncertainties obtained by propagating counting statistic errors through the function that describes the X-ray spectrum [69], are added in quadrature with the uncertainties estimated for ionization cross section, fluorescence yield and detector efficiency. In this approach, all the difficulties inherent to standardless analysis related to instrumental and theoretical parameters are present in the analytical prediction of the spectrum. For the description of the calculated intensities \tilde{I}_i , the last version of POEMA includes a database for K- and L-relative transition probabilities [109–111], for K- and L-ionization cross sections [12], for $K\alpha$ and $K\beta$ satellite lines [112,113], for K-, L- and M-characteristic energies [114], for K- and L- fluorescence yields [115], and for K-, L- and M-shell ionization energies [116,117]. The model of Riveros et al. [118] was implemented for the ionization distribution function while the mass absorption coefficients proposed by Heinrich are used [119]. Bremsstrahlung is accounted for the model given by Castellano and coworkers [120,121] and the line shape for EDS is described according to Visňovezky et al. [13]. A routine for processing WDS spectra was also included, with a proper description for the line shape [15] and detector efficiency [14]. Finally, the effects produced in a spectrum by a possible oxidation layer and by a conductive coating film deposited on the sample were included in the program [122].

4. Precision and accuracy of the different methods

For a proper evaluation of the performance of a quantification method, it is necessary to assess determinations carried out with a large number of samples of known composition involving different experimental situations. In order to test the goodness of each algorithm, histograms obtained from the deviations δ of the calculated concentrations C relative to the nominal values C_n have been widely used [6,21,24]:

$$\delta = (C - C_n) / C_n \times 100$$

The closer the histogram maximum to zero, the better the accuracy of the assessed method. In addition, the histogram width reveals the precision of the algorithms, the narrowest histograms corresponding to the most precise methods. Finally, the number of samples or experimental conditions considered in each test is evidenced by the histogram area, provided the bar width is the same.

Methods applied to the characterization of individual particles will be treated separately from the ones applied to bulk samples, since a better performance can be demanded to the latter.

4.1. Individual particles

Among the methods described above, the ones applied to the characterization of individual particles are those developed by Lábár and Török [17], Trincavelli and Van Grieken [19], and Ro et al. [21].

The first method was tested by using the concentrations calculated for 9 elements in three small fragments taken from the NBS K961 glass standard, amounting to 27 elemental determinations, while the second algorithm was evaluated with 100 determinations carried out in four particle standards, one of them with the same composition as K961. Finally, Ro et al. tested their method using a large number of elemental determinations in particles deposited on Al and Ag substrates, containing elements typical of environmental aerosols. The same algorithm was further assessed by Choël et al. [123] with a B substrate.

In Fig. 1, histograms corresponding to these three methods are shown. For the algorithm developed by Ro et al., only the 375 determinations performed in particles on Al substrate were included (the histogram corresponding to particles on Ag substrate, showed in the original paper, exhibits a similar performance). The scale chosen includes almost

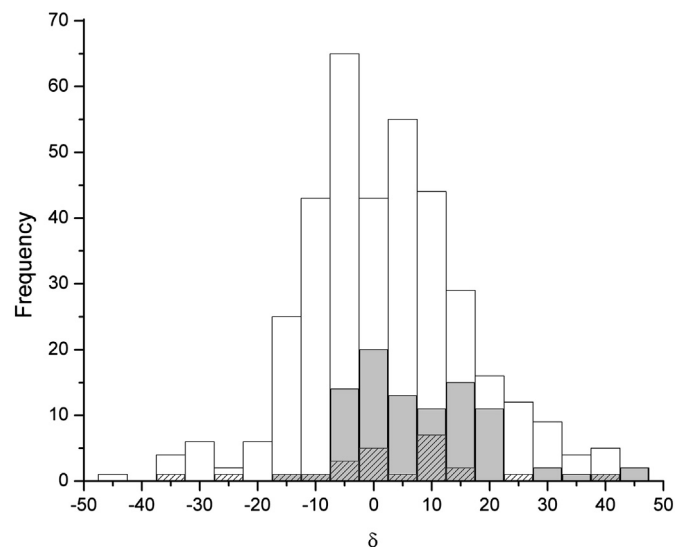


Fig. 1. Histograms of the differences of concentrations relative to the nominal values for standardless quantification methods applied to individual particles. White bars: Ro et al. (Al substrate) [21], gray bars: Trincavelli and Van Grieken [19], dashed bars: Lábár and Török [17].

all the analyses carried out: around 99% for ref. [21], 93% for ref. [19] and 89% for ref. [17].

The deviation from the nominal concentrations is less than 15% for 74% of the concentrations determined by Ro et al. [21] and by Trincavelli and Van Grieken [19], and for 70% of the determinations performed by Lábár and Török [17].

It must be noted that the MC reverse method was optimized for low atomic number elements, which is of interest in the field of environmental studies. On the other hand, the calculation time ranging between 1 and 5 min required to quantify one particle reported in the original article was dramatically improved two years later by Choël et al. [123], who reported a simulation time of a few seconds per particle. The calculations in the other two methods are instead practically instantaneous.

4.2. Bulk samples

Before showing some histograms of the different methods analyzed here, a few remarks will be done about the works published by Steinbrecher [22], Völkerer et al. [92] and Fournier et al. [20].

Steinbrecher evaluated the performance of his MC algorithm for EPMA analysis by studying the spectra of 18 commercial alloys with elements of atomic number between 13 and 29, under different excitation energies, amounting 206 elemental quantifications. Unfortunately, the author does not report neither the nominal concentrations nor the values obtained by him, but only histograms of the differences respect to a reference concentration. For this reason, it was not possible to reconstruct a histogram like the ones presented here for the other methods considered. Nevertheless, an estimation of 0.83% for the precision of the method was given by the author from the deviation of the concentrations respect to the mean value obtained considering different excitation energies. Besides, an accuracy of around 3% was estimated from the deviation of the concentrations relative to the values obtained by two different EPMA standardless quantification methods [18,124].

According to Völkerer et al. [92], their standardless method achieves results with a precision within the range obtained with standards. Particularly, the authors tested this approach in the determination of thin film thickness and composition of binary samples, obtaining an average deviation of less than 10%. Nevertheless, this method is restricted to samples with a combination of appropriate mass absorption coefficients. In fact, for a proper application of the method, two conditions must be fulfilled: firstly, the characteristic line of interest must suffer a high attenuation in the other elements, and secondly, this attenuation must be quite different from the self-attenuation.

In addition, Fournier et al. tested their method by analyzing only two samples: andradite [20] and a $\text{UO}_2\text{-ZrO}_2$ matrix in a corium sample [102]. In the first case, the authors report the deviation of measured and calculated intensities, which reach 9% for one of the elements considered. For the other sample instead, they give the δ value, which is below 3% except for a trace element present in a concentration of 1%. The poor statistical significance of this evaluation does not allow a comparison with the other methods studied here.

The standardless methods to be compared in this work for bulk samples are the approaches implemented in the programs DTSA [6], POEMA and GENESIS SPECTRUM® (EDAX) [125], as well as the algorithms reported by Wernisch [18], Horny et al. [23], and Heckel and Jugelt [16] (see Fig. 2).

The scale chosen for the abscissas includes most of the analyses carried out: all the data reported in Refs. [16] and [23], around 97.5% of the analyses for POEMA [24], 97% for GENESIS [24,125] and 84.5% for DTSA [6]. It must be noted that the histogram reported by Wernisch in his original paper does not detail data beyond 20%, thus, the number of analyses performed with this algorithm lying within the scale shown in Fig. 2 cannot be assured.

The database used by Wernisch [18] includes the greatest number of analyses (580 determinations). The histograms corresponding to the

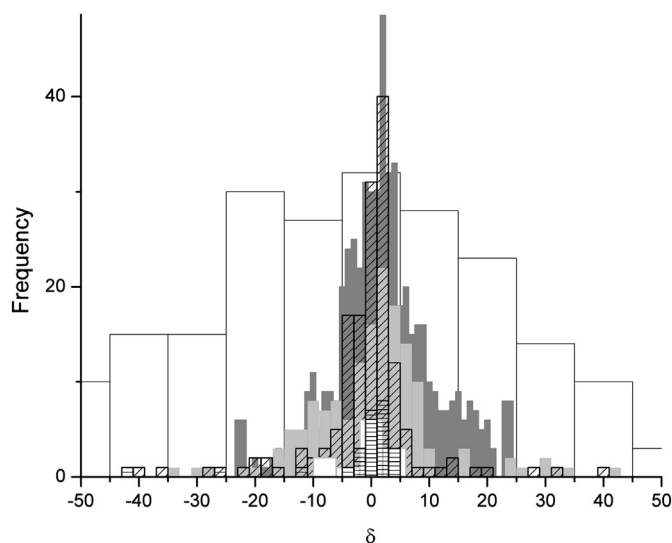


Fig. 2. Histograms of the differences of concentrations relative to the nominal values for standardless quantification methods applied to bulk samples. White and wide bars: DTSA [6], dark gray bars: Wernisch [18], light gray bars: GENESIS [24], diagonal line bars: POEMA [24], white and narrow bars: Horny et al. [23], horizontal line bars: Heckel and Jugelt [16].

evaluation of the DTSA software package [6], the POEMA software and the GENESIS commercial package [24,125] are also quite comprehensive, including 238, 159 and 158 individual determinations, respectively. Instead, the models developed by Horny et al. [23] and Heckel and Jugelt [16] were tested with less data, as can be seen in Table 1.

It is important to analyze the characteristics of the set of samples used to test each method. Besides the number of determinations, different features must be considered. For instance, the number of trace elements, i.e., those with mass concentration lower than 1%, the number of elements in each sample, if low Z elements are considered, if L or M lines are used for the analysis, etc. In Table 1, the main characteristics of the databases used to test each method are shown, along with an estimation of their accuracy.

A deviation from the nominal concentrations less than 10% is observed for 84% of the values determined with POEMA, 76% determined with GENESIS, 75% determined by Wernisch, and only 25% determined with DTSA. Regarding the methods with less individual determinations, all the concentrations calculated by Horny et al., and 88% determined by Heckel and Jugelt deviate by less than 10%. The only methods in the first group for which trace elements are analyzed are POEMA and GENESIS (Wernisch reports only one trace analysis in the original paper); regarding the second group, Heckel and Jugelt analyzed four trace elements.

According to the results shown in Table 1, standardless methods present errors considerably greater than the ones arising when methods

with standards are used. Thus, the analysis carried out with standards is preferable, whenever possible.

In this regard, Newbury [6,126,127] emphasizes the risk of using standardless methods, due to the large uncertainties involved. This is particularly true for the methods that force results to add up 100%, for which the sum of calculated concentrations cannot be used as a quality criterion for the analysis. However, due to successive efforts made to improve the description of generation, absorption and detection of X-rays, the performance of standardless methods has increasingly been improved. Particularly, if traces are disregarded, a remarkable improvement in the performance of the most recent methods can be noticed with respect to the earlier algorithms, as can be seen in the eighth column of Table 1, where a δ value close to 10% is achieved for POEMA. It must be stressed that this software allows for the estimation of uncertainties; moreover, it can be seen that for 81% of the analyses shown in ref. [24] the difference ΔC between calculated and nominal concentrations is lower than the error σ estimated, while for 96% of the determinations ΔC is lower than 3σ . These figures suggest that the estimation of errors performed by this method is adequate.

5. Conclusion

Several standardless algorithms for EPMA quantification were discussed as well as their accuracy. They were classified into five different groups: methods using databases or stored standards, those based on peak-to-background ratios, other ones involving Monte Carlo simulations, one method related to variable take-off angle, and some other methods consisting on the application of fundamental equations of microanalysis.

Although the methods with standards are more reliable, some of the standardless algorithms available nowadays give results with sufficient level of accuracy for many practical applications, even achieving a relative difference between calculated and nominal concentrations close to 10% for 95% of the analyses, when traces are excluded.

Care must be taken with results provided by standardless methods that normalize the calculated concentration values to 100%, unless an estimate of the errors is reported. To the best of the authors' knowledge, only one of the standardless methods gives an adequate estimation of the associated errors, by propagating the counting statistical errors through the function that describes the X-ray spectrum, and adding in quadrature the estimated uncertainties for ionization cross section, fluorescence yield and detector efficiency.

Due to the important improvement in the accuracy and precision achieved in the last years, standardless algorithms have become an interesting alternative for the user when no suitable set of standards is available, also for the analysis of rough samples, and even to avoid the problem caused by large current fluctuations, e.g., for scanning electron microscopes with cold field emission guns.

Nevertheless, to achieve an accuracy closer to the one obtained with methods that use standards, it is necessary to improve even more

Table 1

Main characteristics of the databases used to test each method and the corresponding estimator of accuracy δ . The total number of analyses and the number of trace elements are shown in the second and third columns, respectively. The fourth column indicates if elements with $Z < 9$ are considered, whereas the fifth column shows the spectral lines used. In the sixth column the average number of elements analyzed per sample is displayed. The two following columns show the δ value for which 95% of the determinations are included, considering all the analyses and excluding trace elements. The last column refers to the kind of spectrometer (EDS or WDS) for which the method is applicable.

Method	Analyses	Traces	Light elements	Lines	Analyzed elements	δ for 95% of data (all)	δ for 95% of data (no traces)	Spectrom.
POEMA	159	26	Yes	K ^a	4.4	14%	11.5%	EDS ^c
GENESIS	158	25	Yes	K ^b	4.4	28%	16.5%	EDS
Ref. [18]	580	1	No	K, L	2.7	21%	21%	EDS WDS
DTSA	238	0	No	K, L, M	3	80%	80%	EDS
Ref. [23]	12	0	No	K, L, M	2	8.5%	8.5%	EDS
Ref. [16]	25	4	No	K, L	2.3	26%	4%	EDS

^a It allows the use of L lines for quantification, but they were not used in the present test.

^b It allows the use of L and M lines for quantification, but they were not used in the present test.

^c It works also with WDS spectra, but they were not used in the present test.

the description of the spectrometer efficiency, and of certain atomic parameters like ionization cross sections and fluorescence yields, especially for L and M lines.

References

- [1] R. Castaing, A. Guinier, Application des sondes électroniques à l'analyse métallographique, in: M. Nijhoff (Ed.), Proceedings of the Conference on Electron Microscopy, The Hague, 1950, pp. 60–63.
- [2] R. Castaing, Application des sondes électroniques a une methode d'analyse ponctuelle chimique et crystallographique, (PhD Thesis) University of Paris, 1951.
- [3] R. Fitzgerald, K. Keil, K.F.J. Heinrich, Solid-state energy-dispersion spectrometer for electron-microprobe X-ray analysis, *Science* 159 (1968) 528–530.
- [4] J. Goldstein, D. Newbury, D. Joy, C. Lyman, P. Etchling, E. Lifshin, L. Sawyer, J. Michael, Scanning electron microscopy and X-ray microanalysis, third ed. Springer, New York, 2007.
- [5] J.S.B. Reed, Electron microprobe analysis and scanning electron microscopy in geology, Cambridge University Press, Cambridge, 1996.
- [6] D. Newbury, C. Swyt, R. Myklebust, "Standardless" quantitative electron probe microanalysis with energy-dispersive X-ray spectrometry: is it worth the risk? *Anal. Chem.* 67 (1995) 1866–1871.
- [7] C. Merlet, Capability and uncertainty of standardless procedures for quantitative electron probe X-ray microanalysis, *Microsc. Microanal.* 9 (2003) 524–525.
- [8] R. Gauvin, What remains to be done to allow quantitative X-ray microanalysis performed with EDS to become a true characterization technique? *Microsc. Microanal.* 18 (2012) 915–940.
- [9] J. Pouchou, Standardless X-ray analysis of bulk specimens, *Microchim. Acta* 1 (1994) 33–52.
- [10] M. Procop, Measurement of X-ray emission efficiency for K-lines, *Microsc. Microanal.* 10 (2004) 481–490.
- [11] M. Alvisi, M. Blome, M. Griepentrog, V.-D. Hodoroaba, P. Karduck, M. Mostert, M. Nacucchi, M. Procop, M. Rohde, F. Scholze, P. Statham, R. Terborg, J.-F. Thiot, The determination of the efficiency of energy dispersive X-ray spectrometers by a new reference material, *Microsc. Microanal.* 12 (2006) 406–415.
- [12] C.S. Campos, M.A.Z. Vasconcellos, J.C. Trincavelli, S. Segui, Analytical expression for K- and L-shell cross sections of neutral atoms near ionization threshold by electron impact, *J. Phys. B: At. Mol. Opt. Phys.* (2007) 3835–3841.
- [13] C. Visňovezky, S. Limandri, M. Canafoglia, R. Bonetto, J. Trincavelli, Asymmetry of characteristic X-ray peaks obtained by a Si(Li) detector, *Spectrochim. Acta Part B* 62 (2007) 492–498.
- [14] J. Trincavelli, S. Limandri, A. Carreras, R. Bonetto, Experimental method to determine the absolute efficiency curve of a wavelength dispersive spectrometer, *Microsc. Microanal.* 14 (2008) 306–314.
- [15] S. Limandri, R. Bonetto, H. Di Rocco, J. Trincavelli, Fast and accurate expression for the Voigt function. Application to the determination of uranium M linewidths, *Spectrochim. Acta B* 63 (2008) 962–967.
- [16] J. Heckel, P. Jugelt, Quantitative analysis of bulk samples without standards by using peak-to-background ratios, *X-Ray Spectrom.* 13 (1984) 159–165.
- [17] J. Lábár, S. Török, A peak-to-background method for electron probe X-ray microanalysis applied to individual small particles, *X-Ray Spectrom.* 21 (1992) 183–190.
- [18] J. Wernisch, Quantitative electron microprobe analysis without standard samples, *X-Ray Spectrom.* 14 (1985) 109–119.
- [19] J. Trincavelli, R. Van Grieken, Peak-to-background method for standardless electron microprobe analysis of particles, *X-Ray Spectrom.* 23 (1994) 254–260.
- [20] C. Fournier, C. Merlet, O. Dugne, M. Fialin, Standardless semi-quantitative analysis with WDS-EPMA, *J. Anal. At. Spectrom.* 14 (1999) 381–386.
- [21] C.U. Ro, J. Osán, I. Szaloki, J. de Hoog, A. Worobiec, R. Van Grieken, A Monte Carlo program for quantitative electron-induced X-ray analysis of individual particles, *Anal. Chem.* 75 (2003) 851–859.
- [22] S. Steinbrecher, A unified Monte Carlo approach for quantitative standardless X-ray fluorescence and electron probe microanalysis inside the scanning electron microscope, (PhD Thesis) der Eberhard-Karls-Universität Tübingen, 2004.
- [23] P. Horny, E. Lifshin, H. Campbell, R. Gauvin, Development of a new quantitative X-ray method for electron microscopy, *Microsc. Microanal.* 16 (2010) 821–830.
- [24] S.P. Limandri, R.D. Bonetto, V. Galván Josa, A.C. Carreras, J.C. Trincavelli, Standardless quantification by parameter optimization in electron probe microanalysis, *Spectrochim. Acta B* 77 (2012) 44–51.
- [25] V. Ambrose, C. Quarles, R. Ambrose, Thin-target bremsstrahlung at 0° from 50 keV electrons, *Nucl. Instrum. Methods Phys. Res., Sect. B* 124 (1997) 457–463.
- [26] S. Portillo, C. Quarles, Absolute doubly differential cross sections for electron bremsstrahlung from rare gas atoms at 28 and 50 keV, *Phys. Rev. Lett.* 91 (2003) 173–201.
- [27] R. Ambrose, D. Kahler, H. Lehtihet, C. Quarles, Angular dependence of thick-target bremsstrahlung, *Nucl. Instrum. Methods Phys. Res., Sect. B* 56 (1993) 327–329.
- [28] M. Semaan, C. Quarles, A model for low energy thick-target bremsstrahlung produced in a scanning electron microscope, *X-Ray Spectrom.* 30 (2001) 37–43.
- [29] E. Acosta, X. Llovet, F. Salvat, Monte Carlo simulation of bremsstrahlung emission by electrons, *Appl. Phys. Lett.* 80 (2002) 3228–3230.
- [30] F. Salvat, J.M. Fernández-Varea, J. Sempau, X. Llovet, Monte Carlo simulation of bremsstrahlung emission by electrons, *Rad. Phys. Chem.* 75 (2006) 1201–1219.
- [31] J. Small, S. Leigh, D. Newbury, R. Myklebust, Modeling of the bremsstrahlung radiation produced in pure-element targets by 10–40 keV electrons, *J. Appl. Phys.* 61 (1987) 459–469.
- [32] J. Trincavelli, G. Castellano, J. Riveros, Model for the bremsstrahlung spectrum in EPMA. Application to standardless quantification, *X-Ray Spectrom.* 27 (1998) 81–86.
- [33] G. Castellano, J. Osán, J. Trincavelli, Analytical model for the bremsstrahlung spectrum in the 0.25–20keV photon energy range, *Spectrochim. Acta B* 59 (2004) 313–319.
- [34] J. Trincavelli, G. Castellano, The prediction of thick target electron bremsstrahlung spectra in the 0.25–50 keV energy range, *Spectrochim. Acta B* 63 (2008) 1–8.
- [35] J. Santos, F. Parente, Y. Kim, Cross sections for K-shell ionization of atoms by electron impact, *J. Phys. B: At. Mol. Opt. Phys.* 36 (2003) 4211–4224.
- [36] S.P. Khare, V. Saksena, J.M. Wadehra, K-shell ionization of atoms by electron and positron impact, *Phys. Rev. A: At. Mol. Opt. Phys.* 48 (1993) 1209–1213.
- [37] P. Barlett, A. Stelbovics, Electron-impact ionization cross sections for elements $Z = 1$ to $Z = 54$, *At. Data Nucl. Data Tables* 86 (2004) 235–265.
- [38] D. Bote, F. Salvat, A. Jablonski, C. Powell, Cross sections for ionization of K, L and M shells of atoms by impact of electrons and positrons with energies up to 1 GeV: analytical formulas, *At. Data Nucl. Data Tables* 95 (2009) 871–909.
- [39] N. Tiwari, S. Tomar, K-shell ionization cross sections of light atoms due to electron impact, *J. At. Mol. Sci.* 2 (2011) 109–116.
- [40] S. Segui, M. Dingfelder, F. Salvat, Distorted-wave calculation of cross sections for inner shell ionization by electron and positron impact, *Phys. Rev. A: At. Mol. Opt. Phys.* 67 (2003) 1–12 (062710).
- [41] J. Eichler, Lectures on ion-atom collisions: from nonrelativistic to relativistic velocities, 1st ed. Elsevier, Amsterdam, 2005.
- [42] C. Hombourger, An empirical expression for K-shell ionization cross section by electron impact, *J. Phys. B: At. Mol. Opt. Phys.* 31 (1998) 3693–3702.
- [43] A.K.F. Haque, M.A. Uddin, A.K. Basak, K.R. Karim, B.C. Saha, Empirical model for the electron-impact K-shell-ionization cross sections, *Phys. Rev. A: At. Mol. Opt. Phys.* 73 (2006) 1–7 (012708).
- [44] M. Talukder, S. Bose, S. Takamura, Calculated electron impact K-shell ionization cross sections for atoms, *Int. J. Mass Spectrom.* 269 (2008) 118–130.
- [45] H. Platten, G. Schiwietz, G. Nolte, Cross sections for K-shell ionization of Si and Ar by 4 keV to 10 keV electron impact, *Phys. Lett. A* 107 (1985) 83–86.
- [46] A. Shchagin, V. Pristupa, N. Khizhnyak, K-shell ionization cross section of Si atoms by relativistic electrons, *Nucl. Instrum. Methods Phys. Res., Sect. B* 84 (1994) 9–13.
- [47] F. He, F. Peng, X. Long, Z. Luo, Z. An, K-shell ionization cross sections by electron bombardment at low energies, *Nucl. Instrum. Methods Phys. Res., Sect. B* 129 (1997) 445–450.
- [48] Z. An, M. Liu, Y. Fu, Z. Luo, C. Tang, C. Li, B. Zhang, Y. Tang, Some recent progress on the measurement of K-shell ionization cross-sections of atoms by electron impact: Application to Ti and Cr elements, *Nucl. Instrum. Methods Phys. Res., Sect. B* 207 (2003) 268–274.
- [49] S.P. Limandri, M.A.Z. Vasconcellos, R. Hinrichs, J.C. Trincavelli, Experimental determination of cross sections for K-shell ionization by electron impact for C, O, Al, Si, and Ti, *Phys. Rev. A: At. Mol. Opt. Phys.* 86 (2012) 1–10 (042701).
- [50] D. Bote, F. Salvat, Calculations of inner-shell ionization by electron impact with the distorted-wave and plane-wave Born approximations, *Phys. Rev. A: At. Mol. Opt. Phys.* 77 (2008) 1–24 (042701).
- [51] A.K.F. Haque, M. Shahjahan, M.A. Uddin, M.A.R. Patoary, A.K. Basak, B.C. Saha, F.B. Malik, Generalized Kolbenstvedt model for electron impact ionization of the K-, L- and M-shell ions, *Phys. Scr.* 81 (2010) 1–12 (045301).
- [52] J.M. Fernández-Varea, S. Segui, M. Dingfelder, L α , L β , and L γ X-ray production cross sections of Hf, Ta, W, Re, Os, Au, Pb, and Bi by electron impact: comparison of distorted-wave calculations with experiment, *Phys. Rev. A: At. Mol. Opt. Phys.* 83 (2011) 1–8 (022702).
- [53] C.S. Campos, M.A.Z. Vasconcellos, X. Llovet, F. Salvat, Measurements of L-shell x-ray production cross sections of W, Pt, and Au by 10–30-keV electrons, *Phys. Rev. A: At. Mol. Opt. Phys.* 66 (2002) 1–9 (012719).
- [54] Y. Wu, Z. An, M.T. Liu, Y.M. Duan, C.H. Tang, Z.M. Luo, Measurements of L-shell x-ray production cross-sections of Au and Ag by low energy electron impact, *J. Phys. B: At. Mol. Opt. Phys.* 37 (2004) 4527–4537.
- [55] Y. Wu, Z. An, Y.M. Duan, M.T. Liu, C.H. Tang, Measurements of L α , L β x-ray production cross sections of Pb by 16–40 keV electron impact, *J. Phys. B: At. Mol. Opt. Phys.* 40 (2007) 735–742.
- [56] Y. Wu, Z. An, Y.M. Duan, M.T. Liu, Measurements of L-shell x-ray production cross-sections of Gd and W by low energy electron impact, *J. Phys. B: At. Mol. Opt. Phys.* 43 (2010) 1–4 (135206).
- [57] Y. Wu, Z. An, Y.M. Duan, M.T. Liu, Measurements of L α , L β x-ray production cross sections of Bi by 17–40 keV electron impact, *Nucl. Instrum. Methods Phys. Res., Sect. B* 268 (2010) 2473–2476.
- [58] Y. Wu, Z. An, Y.M. Duan, M.T. Liu, J. Wu, K-shell ionization cross sections of Cl and L α , L β x-ray production cross sections of Ba by 6–30 keV electron impact, *Nucl. Instrum. Methods Phys. Res., Sect. B* 269 (2011) 117–121.
- [59] A. Moy, C. Merlet, X. Llovet, O. Dugne, Measurements of absolute L- and M-subshell x-ray production cross sections of Pb by electron impact, *J. Phys. B: At. Mol. Opt. Phys.* 46 (2013) 1–9 (115202).
- [60] X. Llovet, C.J. Powell, F. Salvat, A. Jablonski, Cross sections for inner-shell ionization by electron impact, *J. Phys. Chem. Ref. Data* 43 (2014) 1–105 (013102).
- [61] A. Yagishita, Ionization cross sections of krypton M subshells by electron impact, *Phys. Lett. A* 7 (1981) 30–32.
- [62] H. Berndt, H.J. Hunger, Experimental determination of the M-shell ionization cross section, *Phys. Status Solidi A* 84 (1984) K149–K152.
- [63] G. Apaydin, E. Tıraşo lu, U. Çevik, B. Ertu ral, H. Baltaş, M. Ertu rul, A.I. Kobya, Total M shell X-ray production cross sections and average fluorescence yields in 11 elements from Tm to U at photon energy of 5.96 keV, *Rad. Phys. Chem.* 72 (2005) 549–554.

- [64] C. Merlet, X. Llovet, F. Salvat, Near-threshold absolute M-shell x-ray production cross sections of Au and Bi by electron impact, *Phys. Rev. A: At. Mol. Opt. Phys.* 78 (2008) 1–7 (022704).
- [65] S. Puri, Relative intensities for L_i ($i = 1-3$) and M_i ($i = 1-5$) subshell X-rays, *At. Data Nucl. Data Tables* 93 (2007) 730–741.
- [66] O. Dogan, M. Erturul, Measurement of the L_3 to $M_i N_i$ and O_i subshells radiative transition probabilities of elements in the atomic number range $73 \leq Z \leq 92$, *Phys. Scr.* 70 (2004) 283–287.
- [67] O. Simsek, Measurement of probabilities of radiative vacancy transfer from the L_3 subshell to the M shell and the N shell for Pb, Th and U, *J. Phys. B: At. Mol. Opt. Phys.* 35 (2002) 1045–1050.
- [68] O. Simsek, D. Karagoz, M. Erturul, Measurement of K to L shell vacancy transfer probabilities for the elements $46 \leq Z \leq 55$ by photoionization, *Spectrochim. Acta B* 58 (2003) 1859–1865.
- [69] R. Bonetto, A. Carreras, J. Trincavelli, G. Castellano, L-shell radiative transition rates by selective synchrotron ionization, *J. Phys. B: At. Mol. Opt. Phys.* 37 (2004) 1477–1488.
- [70] M. Sharma, S. Kumar, P. Singh, S. Puri, N. Singh, Probabilities for radiative vacancy transfer from L_i ($i = 1, 2, 3$) sub-shells to the M, N and higher shells for elements with $77 \leq Z \leq 92$, *J. Phys. Chem. Solids* 66 (2005) 2220–2222.
- [71] E. Bonzi, Measurement of the radiative vacancy transfer probabilities from the L to M and to N shells for W, Re and Pb using synchrotron radiation, *Nucl. Instr. Meth. B* B245 (2006) 363–366.
- [72] A. Raulo, D. Grassi, E. Perillo, L_3 -subshell x-ray emission rates for Dy and Ho, *J. Phys. B: At. Mol. Opt. Phys.* 40 (2007) 2739–2746.
- [73] M.H. Chen, B. Crasemann, M X-ray emission rates in Dirac–Fock approximation, *Phys. Rev. A: At. Mol. Opt. Phys.* 30 (1984) 170–176.
- [74] S. Limandri, J. Trincavelli, R. Bonetto, A. Carreras, Structure of the Pb, Bi, Th and U M X-ray spectra, *Phys. Rev. A: At. Mol. Opt. Phys.* 78 (2008) 1–10 (022518).
- [75] J.L. Campbell, Fluorescence yields and Coster–Kronig probabilities for the atomic L subshells. Part II: the L_1 subshell revisited, *At. Data Nucl. Data Tables* 95 (2009) 115–124.
- [76] J.L. Campbell, Fluorescence yields and Coster–Kronig probabilities for the atomic L subshells, *At. Data Nucl. Data Tables* 85 (2003) 291–315.
- [77] Y. Chauhan, S. Puri, M_i ($i = 1-5$) subshell fluorescence and Coster–Kronig yields for elements with $67 \leq Z \leq 92$, *At. Data Nucl. Data Tables* 94 (2008) 38–49.
- [78] B.L. Henke, E.M. Gullikson, J.C. Davis, X-ray interactions: photoabsorption, scattering, transmission and reflection at 50–30,000 eV, $Z = 1-92$, *At. Data Nucl. Data Tables* 54 (1993) 181–342.
- [79] C.T. Chantler, K. Olsen, R.A. Dragoset, J. Chang, A.R. Kishore, S.A. Kotochigova, D.S. Zucker, X-ray form factor, attenuation and scattering tables (version 2.1), Available: <http://physics.nist.gov/ffast> 2005 (National Institute of Standards and Technology, Gaithersburg, MD. Originally published as C. T. J. Chantler, *Phys. Chem. Ref. Data* 29 (2000), 597–1048; and C. T. J. Chantler, *Phys. Chem. Ref. Data* 24 (1995) 71–643.).
- [80] D.G.W. Smith, S.J.B. Reed, The calculation of background in wavelength-dispersive electron microprobe analysis, *X-Ray Spectrom.* 10 (1981) 198–202.
- [81] C. Merlet, X. Llovet, J.M. Fernández-Varea, Absolute K-shell ionization cross sections and $L\alpha$ and $L\beta_1$ X-ray production cross sections of Ga and As by 1.5–39-keV electrons, *Phys. Rev. A: At. Mol. Opt. Phys.* 73 (2006) 1–10 (062719).
- [82] D. Newbury, N. Ritchie, Is Scanning Electron Microscopy/Energy Dispersive X-ray Spectrometry (SEM/EDS) quantitative? *Scanning* 35 (2013) 141–168.
- [83] J. Small, K. Heinrich, C. Fiori, R. Myklebust, D. Newbury, M. Dilmore, in: O. Johari (Ed.), The production and characterization of glass fibers and spheres for microanalysis, *Scanning Electron Microscopy, SEM Inc., Amf O'Hare, USA, 1978*, pp. 445–454.
- [84] P. Statham, J. Pawley, in: O. Johari (Ed.), A new method for particle x-ray microanalysis based on peak-to-background measurement, *Scanning Electron Microscopy, SEM Inc., Amf O'Hare, USA, 1978*, pp. 469–478.
- [85] J. Pouchou, F. Pichoir, Basic expression of “PAP” computation for quantitative EPMA, in: J. Packwood, R. Brown (Eds.), *Proc. of 11th ICXOM, University of Western Ontario, London, Canada, 1987*, pp. 249–253.
- [86] J. Small, S. Leigh, D. Newbury, R. Myklebust, Modeling of the bremsstrahlung radiation produced in pure-element targets by 10–40 keV electrons, *J. Appl. Phys.* 61 (1987) 459–469.
- [87] F. Eggert, EDX-spectra simulation in electron probe microanalysis. Optimization of excitation conditions and detection limits, *Mikrochim. Acta* 155 (2006) 129–136.
- [88] C. E. Fiori, C. R. Swyt, R. L. Myklebust (1993), National Institute of Standards and Technology, Gaithersburg, MD 20899. Desktop Spectrum Analyzer. US. Patent 529913.
- [89] R.L. Myklebust, D.E. Newbury, The R factor: the X-ray loss due to electron backscatter, in: K.F.J. Heinrich, D.E. Newbury (Eds.), *Electron Probe Quantitation*, Plenum Press, New York, USA, 1991, pp. 177–190.
- [90] P. Hovington, D. Drouin, R. Gauvin, CASINO: a new Monte Carlo code in C language for electron beam interaction -part I: description of the program, *Scanning* 19 (1997) 1–14.
- [91] M. Gryziński, Classical theory of atomic collisions. I. Theory of inelastic collisions, *Phys. Rev.* 138 (1965) A336–A358.
- [92] M. Völkerer, M. Andrae, K. Röhrbacher, J. Wernisch, A new technique for standardless analysis by EPMA-TWIX, *Mikrochim. Acta Supply* 15 (1998) 317–320.
- [93] J. Wernisch, K. Röhrbacher, Standardless analysis, *Mikrochim. Acta Supply* 15 (1998) 307–316.
- [94] G. Love, M.G. Cox, V.D. Scott, A versatile atomic number correction for electron-probe microanalysis, *J. Phys. D* 11 (1978) 7–22.
- [95] G. Love, M.G. Cox, V.D. Scott, A simple Monte Carlo method for simulating electron-solid interactions and its application to electron probe microanalysis, *J. Phys. D* 10 (1977) 7–23.
- [96] J.L. Pouchou, F. Pichoir, Quantitative analysis of homogeneous or stratified microvolumes applying the model “PAP”, in: K.F.J. Heinrich, D.E. Newbury (Eds.), *Electron Probe Quantitation*, Plenum Press, New York, USA, 1991, pp. 31–76.
- [97] K.F.J. Heinrich, H. Yakowitz, Absorption of primary x-rays in electron probe microanalysis, *Anal. Chem.* 47 (1975) 2408–2411.
- [98] C. Merlet, An accurate computer correction program for quantitative electron probe microanalysis, *Mikrochim. Acta* 114 (115) (1994) 363–376.
- [99] H. Bethe, Zur Theorie des Durchgangs schneller Korpuskularstrahlen durch Materie, *Ann. Phys.* 397 (1930) 325–400.
- [100] W. Bambynek, A new evaluation of K-shell fluorescence yields (fit: $K: 5 \leq Z \leq 25$), in: A. Meisel, T. Münzer (Eds.), *X-84 Proc. on X-ray and inner-shell processes in atoms, molecules and solids*, VEB Druckerei, Langensalza, Germany, 1984, p. 1.
- [101] J.H. Hubbell, P.N. Trehan, N. Singh, S. Puri, A review, bibliography, and tabulation of K, L, and higher atomic shell X-ray fluorescence yields, *J. Phys. Chem. Ref. Data* 23 (1994) 339–364.
- [102] C. Fournier, C. Merlet, P.F. Staub, O. Dugne, An expert system for EPMA, *Mikrochim. Acta* 132 (2000) 531–539.
- [103] G. Cliff, G. Lorimer, The quantitative analysis of thin specimen, *J. Microsc.* 103 (1975) 203–207.
- [104] R. Gauvin, E. Lifshin, H. Demers, P. Horny, H. Campbell, Win X-ray, a new Monte Carlo program that computes X-ray spectrum obtained with a scanning electron microscope, *Microsc. Microanal.* 12 (2006) 49–64.
- [105] H. Rietveld, The crystal structure of some alkaline earth metal uranates of the type M_3UO_6 , *Acta Crystallogr.* 20 (1966) 508–513.
- [106] H. Rietveld, Line profiles of neutron powder-diffraction peaks for structure refinement, *Acta Crystallogr.* 22 (1967) 151–152.
- [107] H. Rietveld, A profile refinement method for nuclear and magnetic structures, *J. Appl. Crystallogr.* 2 (1969) 65–71.
- [108] R. Bonetto, G. Castellano, J. Trincavelli, Optimization of parameters in electron probe microanalysis, *X-Ray Spectrom.* 30 (2001) 313–319.
- [109] G. Castellano, R. Bonetto, J. Trincavelli, M. Vasconcellos, C. Campos, Optimization of K-shell intensity ratios in electron probe microanalysis, *X-Ray Spectrom.* 31 (2012) 184–187.
- [110] J. Trincavelli, G. Castellano, R. Bonetto, L-shell transition rates for Ba, Ta, W, Pt, Pb and Bi using electron microprobe, *Spectrochim. Acta B* 57 (2002) 919–928.
- [111] M. Pia, P. Saracco, M. Sudhakar, Validation of K and L shell radiative transition probability calculations, *IEEE Trans. Nucl. Sci.* 56 (2009) 3650–3661.
- [112] S. Limandri, R. Bonetto, A. Carreras, J. Trincavelli, $K\alpha$ satellite transitions in elements with $12 \leq Z \leq 30$ produced by electron incidence, *Phys. Rev. A: At. Mol. Opt. Phys.* 82 (2010) 1–9 (032505).
- [113] S. Limandri, A. Carreras, R. Bonetto, J. Trincavelli, $K\beta$ satellite and forbidden transitions in elements with $12 \leq Z \leq 30$ induced by electron impact, *Phys. Rev. A: At. Mol. Opt. Phys.* 81 (2010) 1–10 (012504).
- [114] J. Bearden, X-ray wavelengths, *Rev. Mod. Phys.* 39 (1967) 78–124.
- [115] S. Perkins, D. Cullen, M. Chen, J. Hubbell, J. Rathkopf, J. Scofield, Lawrence Livermore National Laboratory Report No. UCRL-50400, vol. 301991.
- [116] J.W. Robinson, *Handbook of Spectroscopy*, vol. 1, CRC Press, Boca Raton, 1974.
- [117] B. Henke, P. Lee, T. Tanaka, R. Shimabukuro, B. Fujikawa, Low-energy x-ray interaction coefficients: photoabsorption, scattering, and reflection: $E = 100-2000$ eV $Z = 1-94$, *At. Data Nucl. Data Tables* 27 (1982) 1–144.
- [118] J. Riveros, G. Castellano, J. Trincavelli, Comparison of $\varphi(\rho z)$ curve models in EPMA, *Mikrochim. Acta* 12 (1992) 99–105.
- [119] K.F.J. Heinrich, Mass absorption coefficients for electron probe microanalysis, in: J. Packwood, R. Brown (Eds.), *Proc. of 11th ICXOM, University of Western Ontario, London, Canada, 1987*, pp. 67–119.
- [120] G. Castellano, J. Osán, J. Trincavelli, Analytical model for the bremsstrahlung spectrum in the 0.25–20 keV photon energy range, *Spectrochim. Acta B* 59 (2004) 313–319.
- [121] J. Trincavelli, G. Castellano, The prediction of thick target electron bremsstrahlung spectra in the 0.25–50 keV energy range, *Spectrochim. Acta B* 63 (2008) 1–8.
- [122] S. Limandri, A. Carreras, J. Trincavelli, Effects of the carbon coating and the surface oxide layer in electron probe microanalysis, *Microsc. Microanal.* 16 (2010) 583–593.
- [123] M. Choël, K. Deboudt, J. Osán, P. Flament, R. Van Grieken, Quantitative determination of low-Z elements in single atmospheric particles on boron substrates by automated scanning electron microscopy-energy-dispersive X-ray spectrometry, *Anal. Chem.* 77 (2005) 5686–5692.
- [124] DX-4 application software package, version 2.11, EDAX International, Mahwah, NJ, USA, 1996.
- [125] SPECTRUM GENESIS, User's manual, Revision 5.10, EDAX Inc., Mahwah, NJ, USA, 2006. (<http://micron.ucr.edu/public/manuals/GenEDS.pdf>).
- [126] D. Newbury, Standardless quantitative electron-excited X-ray microanalysis by energy-dispersive spectrometry: what is its proper role? *Microsc. Microanal.* 4 (1999) 585–597.
- [127] D. Newbury, “Standardless” quantitative electron beam X-ray microanalysis. The situation remains caveat emptor! *Microsc. Microanal.* 8 (Suppl. S02) (2002) 1464–1465.